Multichannel rf-compensated Langmuir probe array driven by a single bias supply

S. J. Jeon, G. S. Eom, J. H. Kim, and W. Choe[a)]
Department of Physics, Korea Advanced Institute of Science and Technology, 373-1 Kusong-dong, Yusong-gu, Taejon 305-701, Korea

(Received 12 April 2001; accepted for publication 22 October 2001)

A multichannel Langmuir probe array driven by a single bias supply was constructed. For the probes to be used in harsh radio frequency (rf) environments, the individual probe has a rf-compensation circuit. For simultaneously obtaining $I-V$ curves from the probe array, shunt resistors were placed between the probe tips and the active terminal of the bias supply. The pickup signal due to the stray capacitance of the signal lines and the shunt resistance is discussed. Modification of the probe bias circuit by utilizing lock-in amplifiers was attempted to obtain the electron energy distribution function. The multichannel probe array and the relevant circuit driven by a single bias supply were successfully tested to obtain plasma parameters from various plasma conditions not only in rf plasma but also in tokamak ohmic plasma.
[DOI: 10.1063/1.1427304]

I. INTRODUCTION

Due to simple and inexpensive construction, Langmuir probes have widely been used in a variety of plasmas ranging from the processing plasmas to the tokamak edge plasmas.[1–6] From the probe measurements, basic but valuable information such as plasma density, temperature, and plasma potential are obtained. The electron energy distribution function (EEDF) can also be inferred from the second derivative of the probe $I-V$ characteristic curve.[7,8]

Especially in the plasmas that are produced by radio frequency (rf) power coupling, care must be taken due to the perturbing effects of the rf interference on the plasma potential which leads to incorrect values of the plasma density and temperature compared with the true values. For example, plasma potential fluctuations are generated through capacitive coupling with the antenna in a transformer-coupled plasma.[4,5] One way to solve the problem is to add an *LC* filter circuit to compensate for the rf effects. In this work we constructed and tested a multichannel rf-compensated Langmuir probe array utilizing a single probe bias supply, aiming not only for diagnosing the rf plasma but also for studying the initial plasma effects on the rf-assisted tokamak plasma startup. Modification of the probe bias circuit was also attempted using lock-in amplifiers to simultaneously obtain the EEDF from the probe array.

II. CIRCUIT DESCRIPTION

Figure 1 shows a schematic diagram of the multichannel rf-compensated Langmuir probe array and its bias circuit for measuring the density and temperature profile on Korea Advanced Institute of Science and Technology (KAIST)-TOKAMAK.[9–11] As the probe bias supply, a 1 A, ±100 V Kepco bipolar operational amplifier (BOP) was used. The ''active'' terminal of the BOP was divided into eight lines to simultaneously drive the probe tips via current-to-voltage converting circuits. The ''common'' terminal of the BOP was connected to the electrical ground of the plasma generation system.

When several probes are employed simultaneously, consideration of electrical grounding is especially important as in other plasma diagnostics. In a tokamak, there are many different kinds of electromagnetic noise sources associated with the use of high magnetic fields and pulse operation of various power sources such as capacitor banks. Under such a harsh environment, it is important for an electronic circuit to have the capability of noise immunity during measurements. One way to accomplish it with regard to using a multichannel probe circuit is to have separate electrical grounds such as the ground of the plasma generation system, the casing ground of the electronic devices, and the signal ground of the data acquisition system. In order to make the ground line impedance as small as possible, cables of large cross-sectional area were used as the ground lines. The electronic circuits were encased by metal shields that were connected to the shielding mesh of the signal line cables. For the signal lines from a function generator to the BOP, twisted two-piece shield cables were used to minimize the noise induced from magnetic flux change.

A shunt resistor for converting the probe current to a voltage signal is commonly placed between the ''common'' terminal of the BOP and the ground of the plasma generation system to obtain the $I-V$ characteristic curve. This scheme has a limitation in that the BOP can drive only a single probe. On the other hand, if the shunt resistors are placed between the ''active'' terminal of the BOP and the probes as shown in Fig. 1, many probes can be driven simultaneously by the single BOP within the limitation of the BOP power capability. In this case, the ground of the data acquisition

[a)]Author to whom correspondence should be addressed; electronic mail: wchoe@mail.kaist.ac.kr

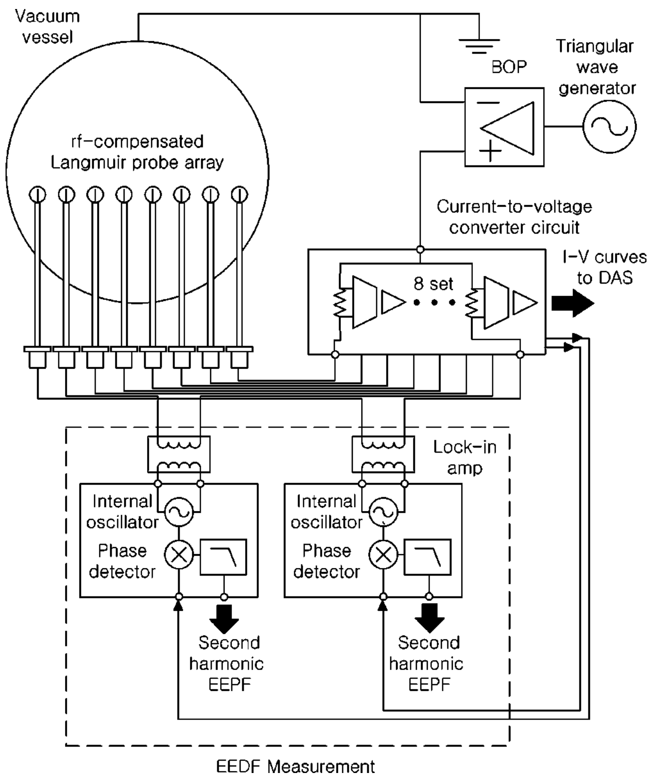

FIG. 1. Schematic diagram of the multichannel Langmuir probe array.

system should not be connected directly to the common point of the shunt resistors because the common voltage varies by hundreds of volts. Therefore the voltage signal across each shunt resistor is acquired through an isolation amplifier which electrically separates the shunt resistor common from the ground of the data acquisition system. The isolation amplifier used for the experiment was AD210, and it provided 2500 V_{rms} and ± 3500 V peak common mode isolation between the probe current pickup port and the signal output port, which is high enough for sweeping the common voltage.

In plasmas produced by rf power coupling, it is known that rf interference significantly affects the probe characteristic. Being different from a dc plasma where the plasma potential is invariant with time, the plasma potential in a rf discharge fluctuates with time often with an amplitude as large as T_e/e where T_e and e are electron temperature and charge, respectively. As a result, the collection current of the probe varies with time due to the fluctuating rf voltage across the probe and the plasma sheath. The fluctuating rf voltage, then, shifts the floating potential and distorts the probe characteristic. Due to this effect, overestimation (underestimation) of the electron temperature (density) inferred by the graphical method based on the distorted $I-V$ curve is brought about compared with the true value. One method to solve the problem is rf compensation by using tuned rf filters.[1–3] A rf-compensated probe consists of a measurement tip, a floating electrode, and rf filters as shown in Fig. 2. The rf filters composed of LC parallel resonant circuits are tuned to the fundamental and the second harmonic frequency of the rf for plasma generation in order to increase the circuit impedance. They are inserted near the probe tip because the

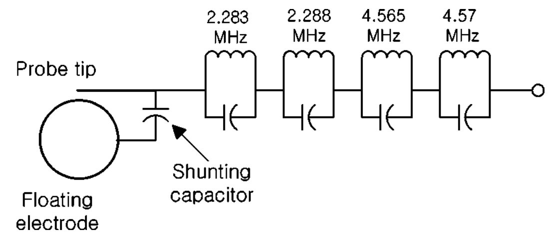

FIG. 2. rf-compensation circuit using a floating electrode and LC resonant filters. The LC resonant filters are tuned to the fundamental and the second harmonic frequency of the rf for plasma generation (2.283 MHz in this case) in order to increase the circuit impedance.

stray capacitance of the lead wire between the probe tip and the rf filters reduces the circuit impedance to the ground. The floating electrode is connected through a shunting capacitor to the measurement tip. Its capacitance is determined in such a way that the impedance of the shunting capacitor is much smaller than the impedance of the plasma sheath at the operation rf frequency. The floating electrode increases the capacitance and reduces the resistance of the sheath, which results in reducing the voltage division ratio of the sheath impedance to the circuit impedance. In this way, the floating electrode and the rf filters cancel the rf voltage fluctuation between the probe tip and the plasma sheath. Since the rf signal contains a large second harmonic, the filters should have resonance at both ω and 2ω where ω is the rf frequency.

For the signal lines from the rf filters to the input of the measurement electronics, coaxial cables were used to reduce capacitive coupling of the rf noise and to provide electromagnetic shielding. By using coaxial cables, the coupling capacitance is reduced approximately as

$$\frac{1}{C_{\mathrm{coupling}}} = \frac{1}{C_{\mathrm{direct}}} + \frac{1}{C_{\mathrm{coax}}}, \tag{1}$$

where C_{direct} is the capacitance between the signal line and the stainless steel tubing which encases the probe when a coaxial cable is not used, and C_{coax} is the capacitance of the coaxial cable.

In the plasmas where high time resolution of the probe measurement is required, it can be accomplished by sweeping the bias voltage from a negative to a positive value, for example, with a triangular wave form. In this case, consideration on the sweeping frequency must be given. As shown in Fig. 3, the shunt resistance R_{shunt} and the stray capacitance of the coaxial cable and the measurement electronics casing C_{stray} form a differential circuit. Thus the shunt resistor ad-

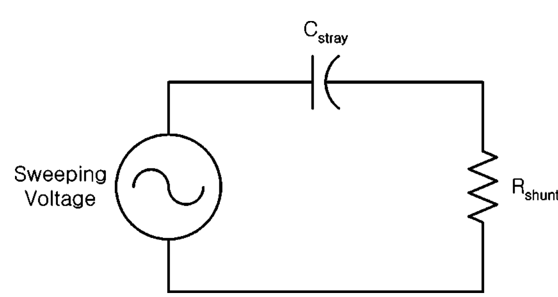

FIG. 3. An equivalent differential circuit consisting of a shunt resistance and the stray capacitance due to the shielding metals and coaxial cables.

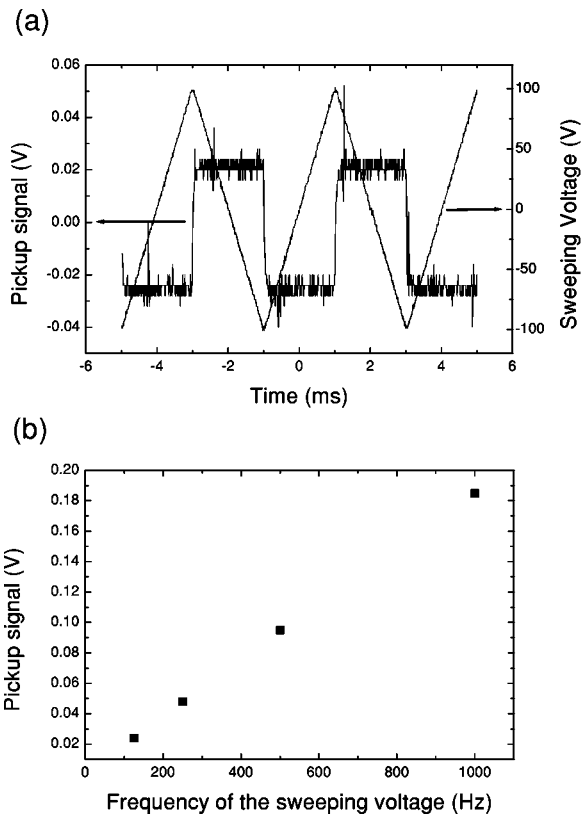

FIG. 4. (a) Differential pickup signal across a 1 kΩ shunt resistor for 500 Hz, 200 V_{pp} sweeping bias voltage. (b) Amplitude of the pickup signal for 125, 250, 500, and 1000 Hz frequencies of the sweeping voltage.

ditionally picks up a voltage that is proportional to the time derivative of the sweeping voltage V_{sweep}, i.e.,

$$V_{\mathrm{pickup}}=R_{\mathrm{shunt}}C_{\mathrm{stray}}\frac{dV_{\mathrm{sweep}}}{dt}. \tag{2}$$

Figure 4(a) shows the sweeping voltage and the differential pickup signal at the 1 kΩ shunt resistor by a 500 Hz, 200 V_{pp} triangular sweeping voltage and a 2 m coaxial cable from the probe tip to the current-to-voltage converter circuit. Equation (2) indicates that the sweeping frequency of the bias voltage should not be too high because the pickup voltage becomes large with respect to the probe output signal. In order to minimize the undesirable pickup voltage, the stray capacitance should be reduced by using short coaxial cables with high characteristic impedance, or by using a small value of the shunt resistor. Figure 4(b) plots the amplitude of the pickup signal for the 125, 250, 500, and 1000 Hz sweeping frequencies of the probe bias voltage. The figure shows that the pickup voltage can also be reduced by choosing as low a sweeping frequency as possible within the experimental conditions.

Conversely, the stray capacitance can be measured from the frequency response of the pickup signal. For instance, the stray capacitance calculated from Eq. (2) with the measured values is about 200 pF. It turns out to be the same as the capacitance of the coaxial cable with 50 Ω characteristic impedance (100 pF/m).

III. EEDF MEASUREMENT

In addition to the $I-V$ characteristic curves, the fabricated rf-compensated probe array is also capable of measuring the EEDF by slight modification of the bias circuit using lock-in amplifiers. The electron energy distribution function f_E is obtained from the second derivative of the collection current with respect to the probe bias voltage.[7,8] The EEDF, electron density, and average electron energy are given as

$$f_E=\epsilon^{1/2}f_P=\frac{4}{A_p e^2}\sqrt{\frac{m_e V_\phi}{2e}}\frac{d^2I}{dV_\phi^2}, \tag{3}$$

$$n_e=\int f_E\, d\epsilon, \tag{4}$$

$$\langle\epsilon\rangle=\eta_e^{-1}\int \epsilon f_E d\epsilon, \tag{5}$$

$$\epsilon=eV_\phi, \tag{6}$$

$$V_\phi=V_{\mathrm{pl}}-V_b, \tag{7}$$

where f_P is the electron probability distribution function, m_e is the electron mass, A_p is the probe tip area, V_b is the probe bias voltage, and V_{pl} is the plasma potential which is determined as the bias voltage of the zero crossing of d^2I/dV_ϕ^2.

In this work we used the harmonic detection technique[7] to obtain the second derivative d^2I/dV_ϕ^2. If a small ac signal $v(t)=v_0\sin\omega t$ is superimposed on the dc probe bias voltage V_b ($v_0\ll V_b$), Taylor expansion of the probe current is expressed as

$$I=I(V_\phi+v)=I(V_\phi)+v_0\sin\omega t\,\frac{dI}{dV_\phi}+\frac{1}{2!}(v_0\sin\omega t)^2\frac{d^2I}{dV_\phi^2}+\cdots. \tag{8}$$

The dominant term of the second harmonic 2ω is given by

$$I_{2\omega}=\left(\frac{v_0^2}{4}\frac{d^2I}{dV_\phi^2}\right)\cos 2\omega t. \tag{9}$$

Therefore the second derivative of the probe current with respect to the bias voltage can be obtained by simply measuring the amplitude of the second harmonic of the superimposed ac signal.

On the bottom side of Fig. 1, the EEDF measurement part added to the bias circuit is depicted. The sinusoidal signal generated by the internal oscillator of a lock-in amplifier is superimposed on the bias signal through a 1:1 transformer. The impedance of the primary winding of the transformer is larger than the output impedance of the internal oscillator at the operating frequency to effectively transfer the reference sine wave. The operating frequency used for the experiment was chosen to be 7.5 kHz because the output bandwidth of the current-to-voltage converter circuit was 20 kHz. The lock-in amplifier is able to process a signal at a multiple of the internal oscillator frequency.

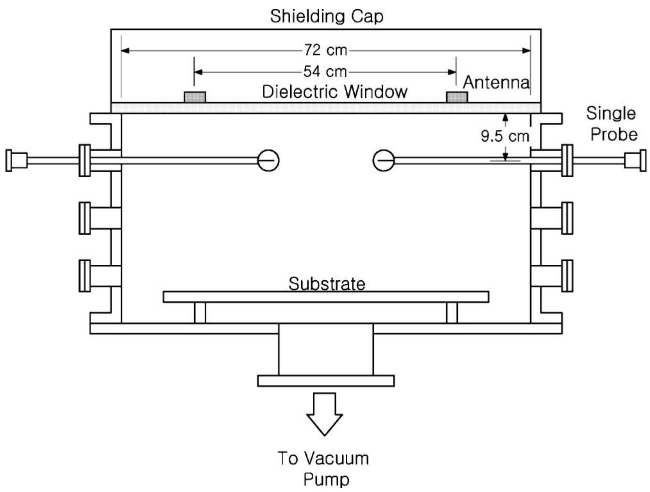

FIG. 5. A schematic drawing of the transformer-coupled plasma source.

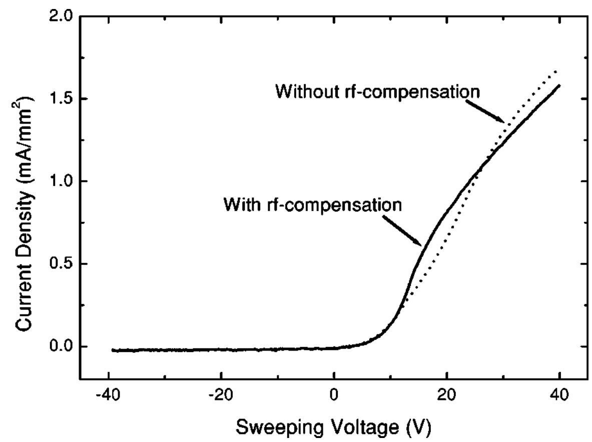

FIG. 6. $I-V$ characteristic curves obtained from a rf-compensated probe and from a bare probe.

IV. EXPERIMENTAL RESULTS

Figure 5 shows the plasma source consisting of a cylindrical chamber of 72 cm diameter, 41 cm height, and a single-turn loop antenna of 54 cm diameter. The operating rf frequency was 2.28 MHz and the helium plasma was produced at 50 mTorr gas pressure. Four rf-compensated probes were installed in the radial direction toward the chamber center and they were located 9.5 cm below the dielectric window. The probes were driven simultaneously by a 1 A, ± 100 V BOP. The tungsten probe tips had 0.5 mm diameter and 10 mm length. The circular-shaped floating electrode was made of a 0.5 mm tungsten wire with 20 mm diameter, which was connected to the probe tip through a 2200 pF capacitor. Two *LC* resonator filters were tuned at slightly different frequencies from each other to provide a wider bandwidth.

One of the $I-V$ characteristic curves obtained from the rf-compensated probes was compared with that acquired from a bare probe which had no rf compensation circuit in order to investigate the effects of the rf on probe measurements. As shown in Fig. 6, the slope of the compensated probe $I-V$ curve is steeper than that of the uncompensated

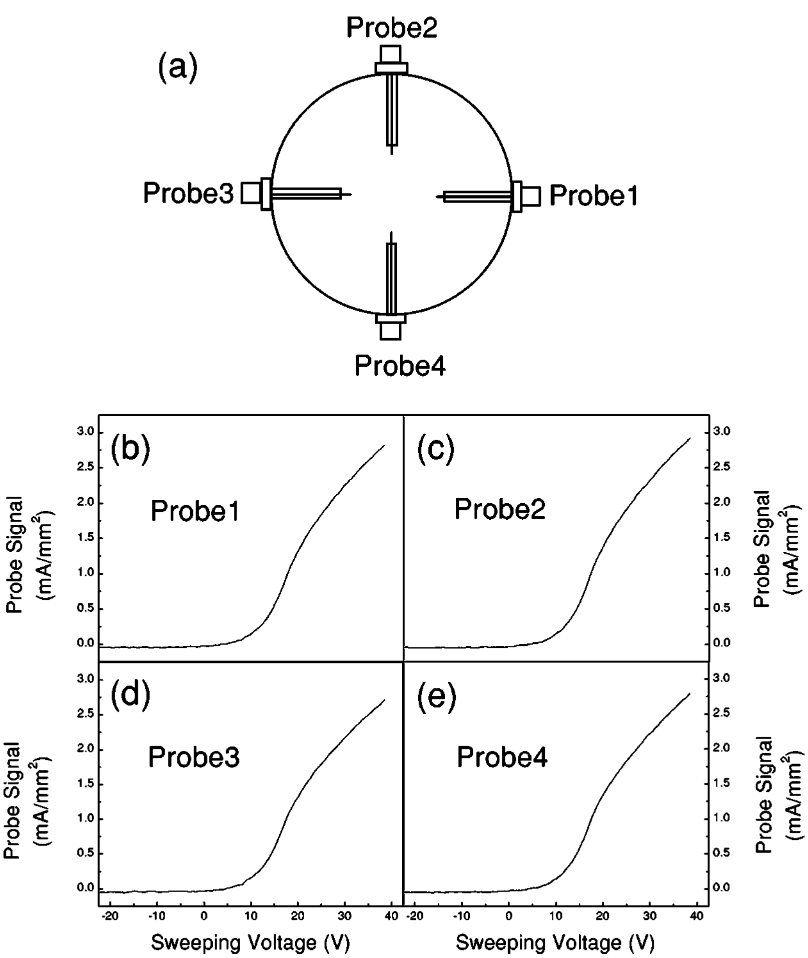

FIG. 7. $I-V$ curves simultaneously acquired by the four probes installed in the transformer-coupled rf plasma source. The probes were located 22 cm from the radial center, 50 Ω shunt resistors were used, and the sweeping frequency of the bias voltage was 125 Hz.

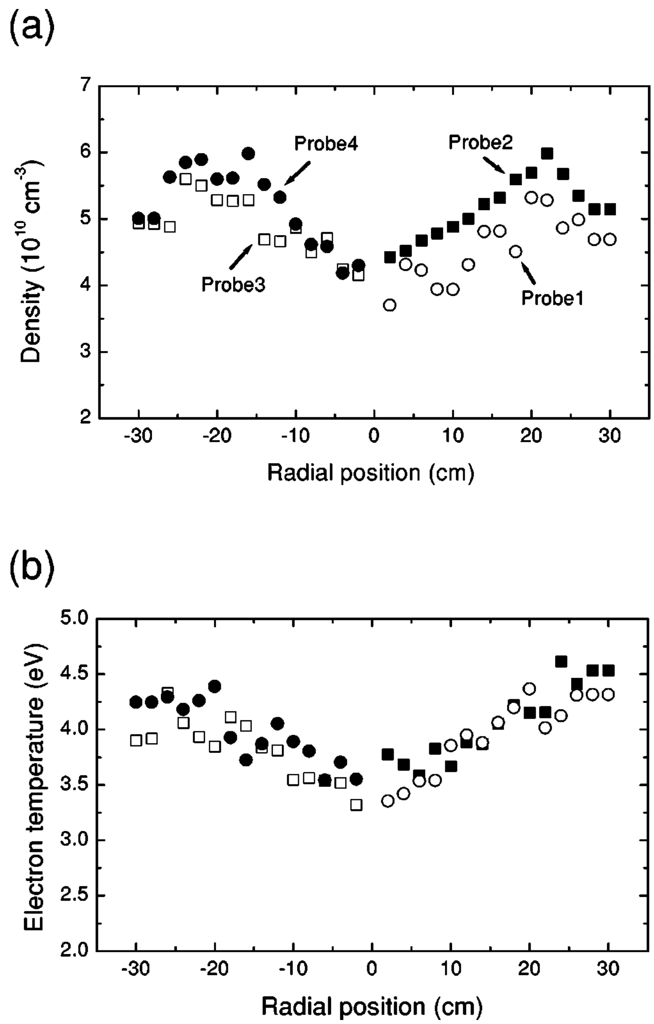

FIG. 8. Radial profiles of the (a) electron density and (b) temperature interpreted from the $I-V$ curves simultaneously acquired by the four Langmuir probes.

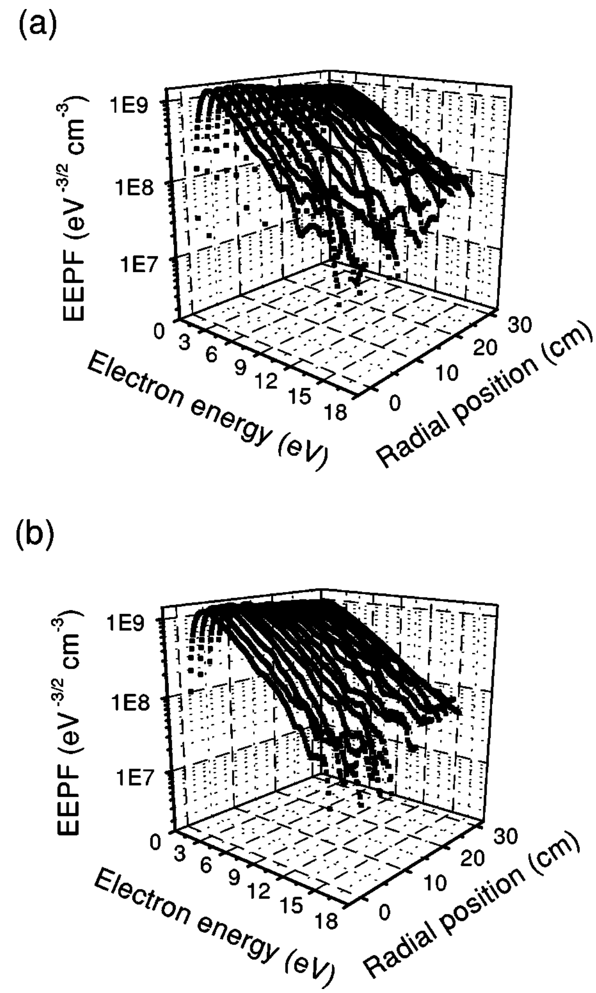

FIG. 9. Radial profiles of the electron probability distribution function obtained simultaneously by two of the probes. The reference sine wave was 1.8 V_{pp} in 7.5 kHz.

one in the electron retardation region. This results in the electron temperature evaluated from the compensated probe to be about 0.5 eV lower than the other, which is about a 15% difference.

The $I-V$ curves that are obtained simultaneously from the four probes are plotted in Fig. 7. In order to have as low pickup voltage as possible originating from the stray capacitance of coaxial cables and the sweeping frequency of the bias voltage, the shunt resistance and the sweeping voltage were chosen as 50 Ω and ±40 V, respectively, with a 125 Hz triangular wave form.

By fitting each of the simultaneously acquired $I-V$ curves at intervals of two centimeters, the plasma density and temperature profiles were obtained, and the results are depicted in Fig. 8. As shown in the figure, the plasma density is about $5\times10^{10}\,\mathrm{cm}^{-3}$ and the electron temperature is about 4 eV. The probes present a similar radial dependence except that probe 1 shows a smaller difference in the density value as compared with the others. It may be attributed to the slight difference in the offset voltage or the probe tip size. The hollow profiles of the density and temperature are due to the fact that the effects of the rf antenna are still strong at the measurement position.

Figure 9 shows two radial profiles of the electron probability distribution function that were simultaneously measured at intervals of two centimeters. It shows that the average electron energy is low (steeper gradient) toward the plasma center, which is already seen in Fig. 8. Although only two channels were attempted at the time of the measurement due to the availability of the lock-in amplifiers, it can easily be extended for more channels.

The developed multichannel probe array was also tested in a tokamak environment. A rf plasma was produced by using a toroidally modified Nagoya type III antenna placed inside the KAIST-TOKAMAK. The vacuum vessel has major and minor radii of 53 and 17 cm, respectively, and the radius of the circular-shaped limiter is 14 cm. The operating rf frequency and power was 13.56 MHz and 1 kW, respectively, and the applied toroidal field was 2.2 kG at the geometric center of the vacuum vessel. The plasma was produced for 200 ms at 0.12 mTorr argon gas pressure. The eight Langmuir probes tuned at 13.56 MHz were installed on the bottom side of the vacuum vessel and were aligned in the major radial direction. The tungsten probe tip had 0.8 mm diameter and 4 mm length. Figure 10 shows the radial profile of the density and temperature on the midplane. To increase the signal-to-noise ratio, the $I-V$ curves were acquired by

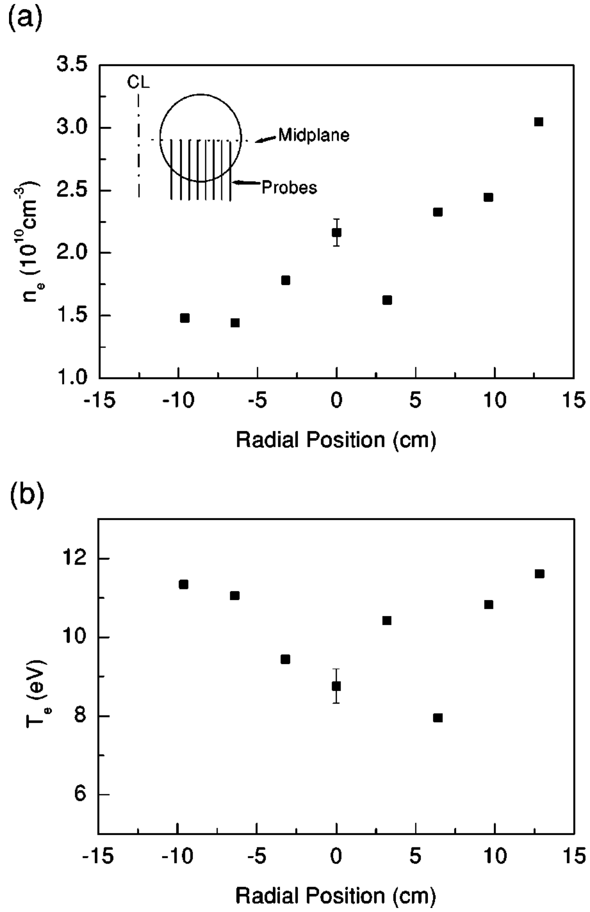

FIG. 10. Radial profile of the (a) electron density and (b) temperature obtained from the $I-V$ curves simultaneously acquired by the eight Langmuir probes. The plasma was produced by 13.56 MHz, 1 kW rf power input using a toroidally modified Nagoya type III antenna. The zero point of the radial axis corresponds to the geometrical center of the KAIST-TOKAMAK vacuum vessel.

averaging 15 data sets. The shunt resistance and the sweeping voltage were chosen as 200 Ω and ± 60 V, respectively, with 100 Hz triangular wave form. The outer region of the density profile is higher, which is consistent with the bright plasma band seen through a quartz window on the outboard side of the midplane. This suggests that the plasma is mainly produced by capacitive coupling with the antenna, resulting in the rather low density and high temperature.

The probe circuit was also applied to a rake probe installed at the edge of the ohmically heated hydrogen plasma on KAIST-TOKAMAK in order to measure the radial profile of the density and temperature. The rake probe having six tungsten tips of 1.2 mm diameter and 3 mm length was installed on the midplane in the major radial direction as shown in Fig. 11 and the tips were aligned perpendicular to the toroidal magnetic field. The edge density and temperature profile of the 18 kA plasma at 4.5 kG toroidal field is plotted in Fig. 11.

In summary, a multichannel rf-compensated Langmuir probe array was constructed by utilizing a single bias supply. The individual probe has a rf-compensation circuit so that it can be used in rf environments. The probe array and the relevant circuit were tested not only in rf plasmas but also in ohmically heated tokamak plasma to find that the developed system is useful for various plasma conditions. By modifying the bias circuit using lock-in amplifiers, it was also demonstrated that several channels of the electron energy distribution function can be simultaneously obtained from the probe array.

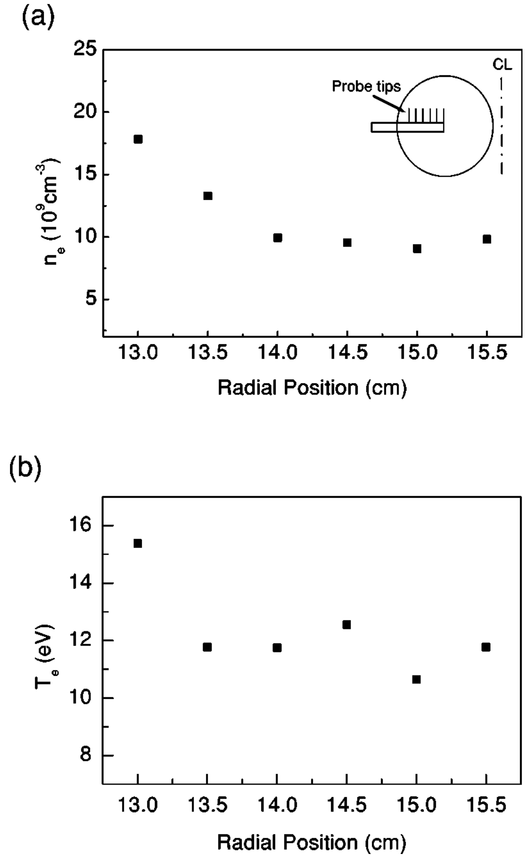

FIG. 11. Radial profile of the (a) electron density and (b) temperature obtained by the six-tip rake probe. The plasma current and toroidal field are 18 kA and 4.5 kG, respectively.

ACKNOWLEDGMENT

This work was supported by Korea Basic Science Institute (KBSI) under the HANBIT User Program and also by the BK21 project.

[1] I. D. Sudit and F. F. Chen, Plasma Sources Sci. Technol. **3**, 162 (1994).
[2] V. A. Godyak, R. B. Piejak, and B. M. Alexandrovich, Plasma Sources Sci. Technol. **1**, 36 (1992).
[3] A. P. Paranjpe, J. P. McVittie, and S. A. Self, J. Appl. Phys. **67**, 6718 (1990).
[4] V. A. Godyak, R. B. Piejak, and B. M. Alexandrovich, J. Appl. Phys. **85**, 703 (1999).
[5] M. Watanabe, D. M. Shaw, G. J. Collins, and H. Sugai, J. Appl. Phys. **85**, 3428 (1999).
[6] R. Back and R. D. Bengtson, Rev. Sci. Instrum. **68**, 377 (1997).
[7] G. R. Branner, E. M. Friar, and G. Medicus, Rev. Sci. Instrum. **34**, 231 (1963).
[8] K. F. Schoenberg, Rev. Sci. Instrum. **49**, 1377 (1978).
[9] W. Choe *et al.*, Rev. Sci. Instrum. **71**, 2728 (2000).
[10] G. C. Kwon *et al.*, Jpn. J. Appl. Phys., Part 1 **39**, 4188 (2000).
[11] S. H. Seo *et al.*, Fusion Technol. **37**, 89 (2000).